



Elucidating the Formation of Ethynylbutatrienylidene (HCCCHCCC; X¹A') in the Taurus Molecular Cloud (TMC-1) via the Gas-phase Reaction of Tricarbon (C₃) with the Propargyl Radical (C₃H₃)

Alexander M. Mebel¹ , Marcelino Agúndez² , José Cernicharo² , and Ralf I. Kaiser³ ¹ Department of Chemistry and Biochemistry, Florida International University, Miami, FL 33199, USA; mebela@fiu.edu² Departamento de Astrofísica Molecular, Instituto de Física Fundamental, Serrano 121, E-28006 Madrid, Spain; marcelino.agundez@csic.es, jose.cernicharo@csic.es³ Department of Chemistry, University of Hawai'i at Manoa, Honolulu, HI 96822, USA; ralfk@hawaii.edu

Received 2022 December 23; revised 2023 February 23; accepted 2023 February 24; published 2023 March 17

Abstract

The recent astronomical detection of ethynylbutatrienylidene (HCCCHCCC)—a high-energy isomer of triacetylene (HCCCCCCH) and hexapentaenylidene (H₂CCCCC)—in TMC-1 puzzled the laboratory astrophysics community since proposed reaction pathways could not synthesize the ethynylbutatrienylidene (HCCCHCCC) under cold molecular cloud conditions. Exploiting a retrosynthesis coupled with electronic structure calculations and astrochemical modeling, we reveal that observed fractional abundance of ethynylbutatrienylidene (HCCCHCCC) of $1.3 \pm 0.2 \times 10^{-11}$ can be quantitatively replicated through the barrierless and exoergic reaction of tricarbon (C₃) with the resonantly stabilized propargyl radical (C₃H₃) after a few 10⁵ yr—typical ages of cold molecular clouds. Our study provides persuasive evidence that previously assumed “dead” reactants such as tricarbon (C₃) and the propargyl radical (C₃H₃) provide fundamental molecular building blocks in molecular mass growth processes leading to exotic, high-energy isomers of hydrocarbons: ethynylbutatrienylidene (HCCCHCCC).

Unified Astronomy Thesaurus concepts: Astrochemistry (75); Interstellar dust (836); Laboratory astrophysics (2004)

1. Introduction

During the last decades, cold molecular clouds such as the Taurus Molecular Cloud (TMC-1) have been recognized as natural laboratories on the macroscopic scale in enriching our knowledge on the molecular inventory of interstellar hydrocarbons—molecules containing only carbon and hydrogen—through astronomical observations exploiting predominantly the Yebes 40 m telescope (Cernicharo et al. 2021a) and the Green Bank 100 m radio telescope (McCarthy & Thaddeus 2002). These C1 to C6 hydrocarbons—among them simple radicals such as methylidyne (CH; Suutarinen et al. 2011) and ethynyl (C₂H; Tucker et al. 1974) along with closed shell species like vinylacetylene (C₄H₄; Cernicharo et al. 2021b)—have emerged as fundamental molecular building blocks to form aromatic molecules, e.g., benzene (C₆H₆; Jones et al. 2011) and naphthalene (C₁₀H₈; Figure 1; Parker et al. 2012). These aromatics were detected astronomically through their cyano derivatives cyanobenzene (C₆H₅CN; McGuire et al. 2018) and 1-/2-cyanonaphthalene (C₁₀H₇CN; McGuire et al. 2021) as products of, e.g., barrierless (Cooke et al. 2020) and exoergic reactions with cyano radicals (CN; Balucani et al. 1999; Kaiser & Balucani 2001) with recent astrochemical models replicating their fractional abundances in TMC-1 *quantitatively* (Kaiser et al. 2022). However, whereas molecular beams studies along with electronic structure calculations provided fundamental knowledge of the elementary reaction mechanisms leading to aromatics in molecular clouds (Kaiser & Hansen 2021), an understanding of the inherent reaction pathways to their C1–C6 hydrocarbon

precursors has not yet been fully accomplished. Similar to complex organic molecules (COMs) in star-forming regions (Turner & Kaiser 2020), structural isomers of hydrocarbons—hydrocarbon molecules with the same molecular formula, but distinct connectivities of the atoms—play a particular role as they act as molecular tracers not only to define the evolutionary stage of molecular clouds, but also to elucidate often isomer-specific reaction pathways in these extreme environments.

The recent detection of the C_s symmetric ethynylbutatrienylidene (HCCCHCCC; X¹A') molecule (Fuentetaja et al. 2022)—an isomer of triacetylene (HCCCCCCH; X¹Σ_g⁺) and the C_{2v} symmetric hexapentaenylidene (H₂CCCCC) (Langer et al. 1997)—in TMC-1 (Figure 2) represents a particular challenge since anticipated bimolecular neutral–neutral reactions of the ethynyl radical (C₂H) with diacetylene (HCCCH) (Reaction (1)) and of the butadiynyl radical (C₄H) with acetylene (C₂H₂) (Reaction (2)) only lead to the microwave inactive triacetylene (HCCCCCCH) isomer (Vakhtin et al. 2001; Landerer et al. 2008; Gu et al. 2009; Berteloite et al. 2010). Therefore, bimolecular and exoergic reactions in the C2–C4 system cannot form the recently detected ethynylbutatrienylidene (HCCCHCCC) molecule



The aforementioned concerns suggest that the formation pathways to newly detected hydrocarbons in TMC-1 cannot be simply *inferred* based on neutral–neutral reactions, but should be elucidated experimentally and/or computationally along with expanded astrochemical models to gain a comprehensive knowledge of the dominating reaction pathways to hydrocarbon (isomers) in molecular clouds. The design of these studies can be

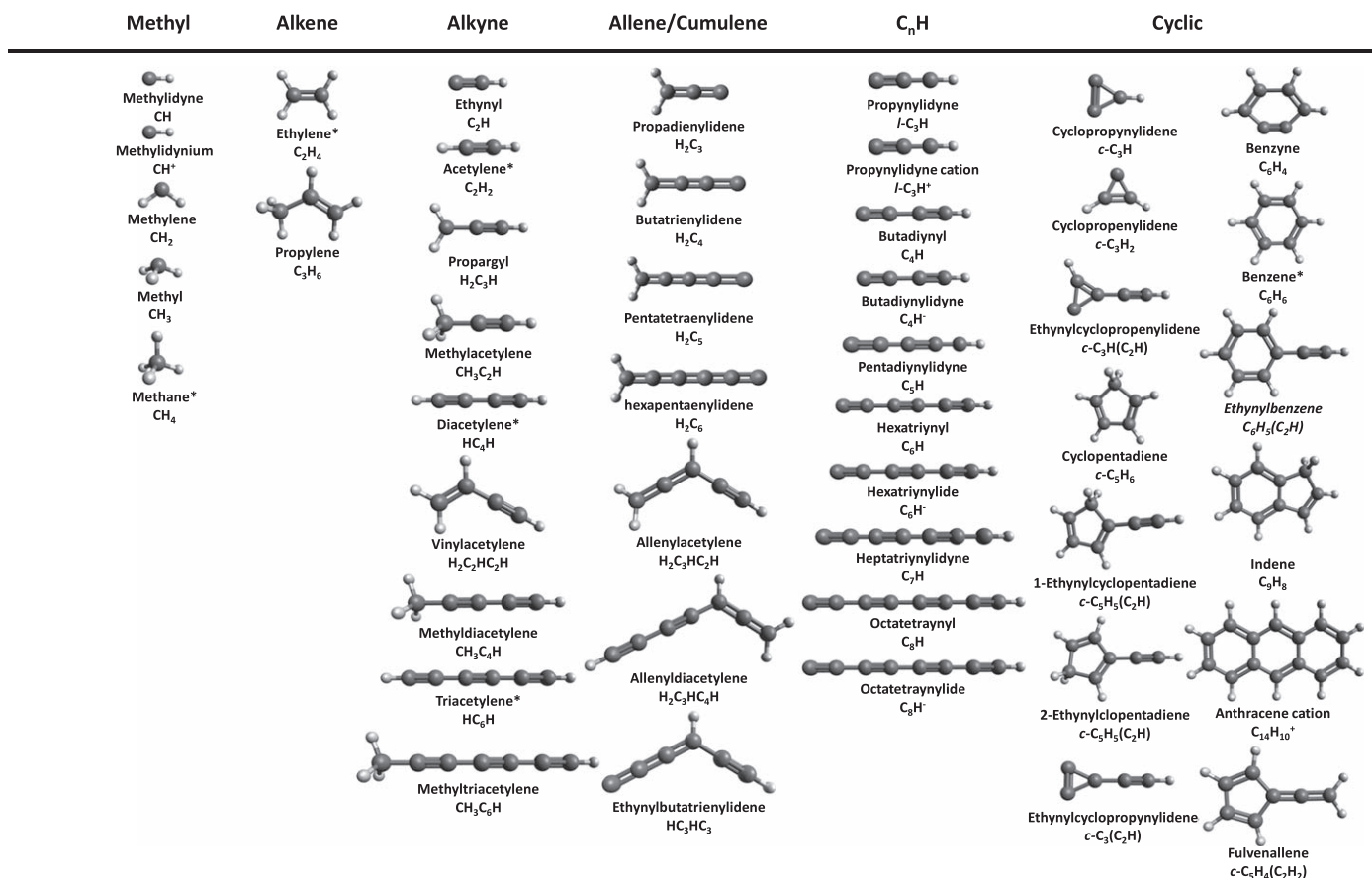


Figure 1. Hydrocarbon molecules detected in circumstellar and interstellar environments. Atoms are color coded in black (carbon) and gray (hydrogen). Molecules only detected in circumstellar envelopes are denoted with an “*.”

guided by a retrosynthesis of the gas-phase molecule of interest by formally decomposing the target molecule (here: ethynylbutatrienylidene (HCCCHCCC)) into fundamental molecular building blocks. This approach reveals three likely gas-phase pathways to ethynylbutatrienylidene (HCCCHCCC): Reaction (3) of the propynylidyne (l-HCCC) radical with propargylene (HCCCH), Reaction (4) of the propynylidyne (l-HCCC) radical with vinylidene carbene (H₂CCC), and the Reaction (5) of tricarbon (C₃) with the propargyl radical (C₃H₃)



All bimolecular gas-phase reactions must be barrierless and exoergic, and potential barriers to isomerization of any reaction intermediate (here: C₆H₃) must be below the energy of the separated reactants (Kaiser 2002). Note that propynylidyne (l-HCCC; Thaddeus et al. 1985), vinylidene carbene (H₂CCC; Cernicharo et al. 1991a), and the propargyl radical (C₃H₃; Agúndez et al. 2021) have been observed in TMC-1 with fractional abundances of $1.1 \pm 0.2 \times 10^{-10}$, $1.8 \pm 0.4 \times 10^{-10}$, and $1.0 \pm 0.2 \times 10^{-8}$, respectively (Loison et al. 2017; Agúndez et al. 2022). Propargylene (HCCCH) has a low dipole moment of only 0.08 Debye and has not been detected yet in TMC-1 (Nguyen et al. 2001), although laboratory experiments merged with computations reveal that the gas-phase reaction of atomic carbon (C(³P)) with vinyl (C₂H₃) (Nguyen et al. 2001; Wilson et al. 2012) and of methyldiyne

(CH) with acetylene (C₂H₂) (Maksyutenko et al. 2011) yield branching ratios of propargylene (HCCCH) of up to $80\% \pm 15\%$ with lower fractions of $15\% \pm 10\%$ and $5\% \pm 3\%$ forming the astronomically detected cyclopropenylidene (c-C₃H₂) and vinylidene carbene (H₂CCC) isomers, respectively.

Here we reveal through a combined computational and astrochemical modeling approach that the gas-phase formation of the recently detected ethynylbutatrienylidene (HCCCHCCC) can be quantitatively explained via the reaction of tricarbon (C₃) with the resonantly stabilized propargyl radical (C₃H₃). The observed fractional abundance of $1.3 \pm 0.2 \times 10^{-11}$ with respect to molecular hydrogen (Fuentetaja et al. 2022) is nicely replicated for TMC-1 models with a simulated peak abundance of close to 1.2×10^{-11} after a few 10^5 yr. Reaction (4) contributes 4 orders of magnitude less to the fractional abundances of ethynylbutatrienylidene (HCCCHCCC) compared to Reaction (5), whereas Reaction (3) forms triacetylene (HCCCCCCH) plus atomic hydrogen, but no ethynylbutatrienylidene (HCCCHCCC). Overall, this study disclosed that previously assumed “dead” reactants such as tricarbon (C₃) and the propargyl radical (C₃H₃) provide fundamental molecular building blocks in molecular mass growth processes leading to exotic, high-energy isomers of hydrocarbons: ethynylbutatrienylidene (HCCCHCCC).

2. Computational

Geometries of all species involved in Reactions (3) to (5) accessing the C₆H₃ potential energy surfaces (PESs) including

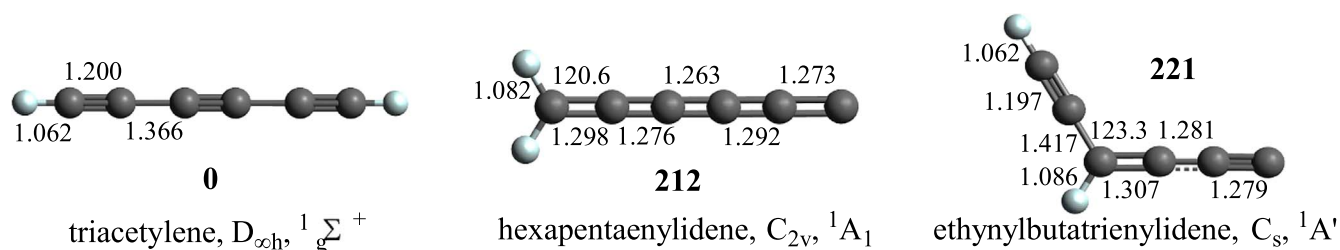


Figure 2. Molecular structures, point groups, electronic wave functions, and relative stabilities of three lowest energy C_6H_2 isomers. Optimized bond lengths are given in Å and angles are given in degrees. Relative energies are shown in bold, in kJ mol^{-1} .

reactants, intermediates, transition states, and reaction products were optimized using the doubly hybrid density functional theory ω B97XD method (Chai & Head-Gordon 2008) with Dunning’s correlation-consistent cc-pVTZ basis set (Dunning 1989). Vibrational frequencies for all optimized structures were computed using the same method to evaluate zero-point vibrational energy corrections (ZPE). Single-point energies were rectified using the explicitly correlated coupled clusters approach with single and double excitations with perturbative treatment of triple excitations, CCSD(T)-F12 (Adler et al. 2007; Knizia et al. 2009), with Dunning’s cc-pVQZ-f12 basis set. The anticipated accuracy of the CCSD(T)-F12/cc-pVQZ-f12// ω B97XD/cc-pVTZ + ZPE (ω B97XD/cc-pVTZ) relative energies is typically within 4 kJ mol^{-1} or better (Zhang & Valeev 2012). The Gaussian 16 (Frisch et al. 2016; He et al. 2022) and MOLPRO 2021 (Werner et al. 2021) program packages were used for the ab initio calculations. Energy-dependent rate constants of all unimolecular reaction steps on the C_6H_3 PES were computed using Rice–Ramsperger–Kassel–Marcus theory (Eyring et al. 1980; Kislov et al. 2004).

3. Astrochemical Modeling

To evaluate to what extent the Reactions (3) to (5) can explain the observed abundances of ethynylbutatrienylidene (HCCCHCCC) of $1.3 \pm 0.2 \times 10^{-11}$ toward TMC-1, chemical modeling calculations were carried out. The physical conditions and chemical network adopted are extracted from Agúndez et al. (2021) to model the abundances of the propargyl radical (C_3H_3). This model was “chemically” updated by including ethynylbutatrienylidene (HCCCHCCC) and formation rates through Reactions (3)–(5) with reaction rates varied from 1 to $4 \times 10^{-10} \text{ cm}^3 \text{ s}^{-1}$. These rates are typical for barrierless and exoergic neutral–neutral reactions at temperatures as low as 10 K (Sims & Smith 1995). Destruction routes for ethynylbutatrienylidene (HCCCHCCC) through reactions involving neutral atoms (H, C, N, O) and abundant cations (C^+ , HCO^+ , H_3O^+ , H_3^+ , H^+) were also added with rate coefficients adopted from the UMIST (McElroy et al. 2013) and KIDA (Wakelam et al. 2015) databases. Note that the reverse reaction of atomic hydrogen with ethynylbutatrienylidene (HCCCHCCC) is barrierless (Section 4, Results and Discussion); this would yield rate coefficients 1 to $4 \times 10^{-10} \text{ cm}^3 \text{ s}^{-1}$; however, statistically, only one out of six collisions of the hydrogen atom with ethynylbutatrienylidene (HCCCHCCC) leads to intermediate **i1**. Therefore, a rate coefficient of $3 \times 10^{-11} \text{ cm}^3 \text{ s}^{-1}$ was adopted.

4. Results and Discussion

To evaluate the potential role of Reactions (3)–(5) in TMC-1, it is important to provide evidence on their barrierless nature, exoergicities, and reaction product(s) (Figures 3(a)–(c) and Figure A1 in the Appendix). The propynylidyne radical (1-HCCC) in its $^2\Pi_{1/2}$ electronic ground state was found to react barrierlessly with the propargylene (HCCCH; X^3B) radical via addition to one of its CH moieties by either its bare C or CH end. This barrierless addition leads to intermediates **i1** and **i2**, which are stabilized by 535 and 396 kJ mol^{-1} relative to the reactants, respectively. In **i1**, atomic hydrogen losses from the terminal carbon atom of the CCCH moiety or from the HC group of propargylene, to which the propynylidyne radical (1-HCCC) added, can form ethynylbutatrienylidene (HCCCHCCC; **p3**) and triacetylene (HCCCCCCH; **p1**) respectively, in bimolecular reactions overall exoergic by 136 and 357 kJ mol^{-1} with respect to the reactants. The initial complex **i2** can directly dissociate only to **p3** via an exit transition state positioned 9 kJ mol^{-1} above the product and 127 kJ mol^{-1} below the reactants but a more favorable pathway involves isomerization of **i2** to **i1** via a 1,3-H migration with the transition state located 204 kJ mol^{-1} below the reactants. Statistical calculations starting from **i1** suggest an exclusive formation of triacetylene (HCCCCCCH; **p1**) under the low-temperature conditions in TMC-1, whereas starting from **i2** the yields of **p3** and **p1** are predicted to be about 2% and 98%, respectively (Table A1).

The bimolecular reaction of the propynylidyne radical (1-HCCC; $X^2\Pi_{1/2}$) with vinylidene carbene (H_2CCC ; X^1A_1) can proceed barrierlessly via additions of the terminal bare or CH-group carbon atoms of the HCCC chain to the carbene carbon atom forming intermediates **i3** and **i4**, respectively, and also via addition of the terminal bare carbon atom of HCCC to the H_2C moiety producing **i5**. These intermediates are energetically favorable by 558, 381, and 120 kJ mol^{-1} with respect to the separated reactants. The initial complex **i3** can directly decompose to triacetylene (HCCCCCCH; **p1**) and hexapentaenylidene (H_2CCCCC ; **p2**) by ejecting atomic hydrogen either from the H_2C moiety of the vinylidene carbene reactant or the CCCH functional group, with the former pathway being much more favorable than the latter. The intermediate **i4** can dissociate only to **p2** but a series of more facile H shifts lead from **i4** to **i3**, **i6**, and **i1**, where the last three isomers predominantly dissociate to triacetylene (HCCCCCCH; **p1**). Alternatively, another hydrogen atom shift can isomerize **i4** to **i7** where the latter can dissociate both to ethynylbutatrienylidene (HCCCHCCC; **p3**) in an overall exoergic reaction (147 kJ mol^{-1}) and to **p2**. From **i5**, an easy hydrogen shift produces **i2**, which can in turn either decompose to **p3** or isomerize to **i1**,

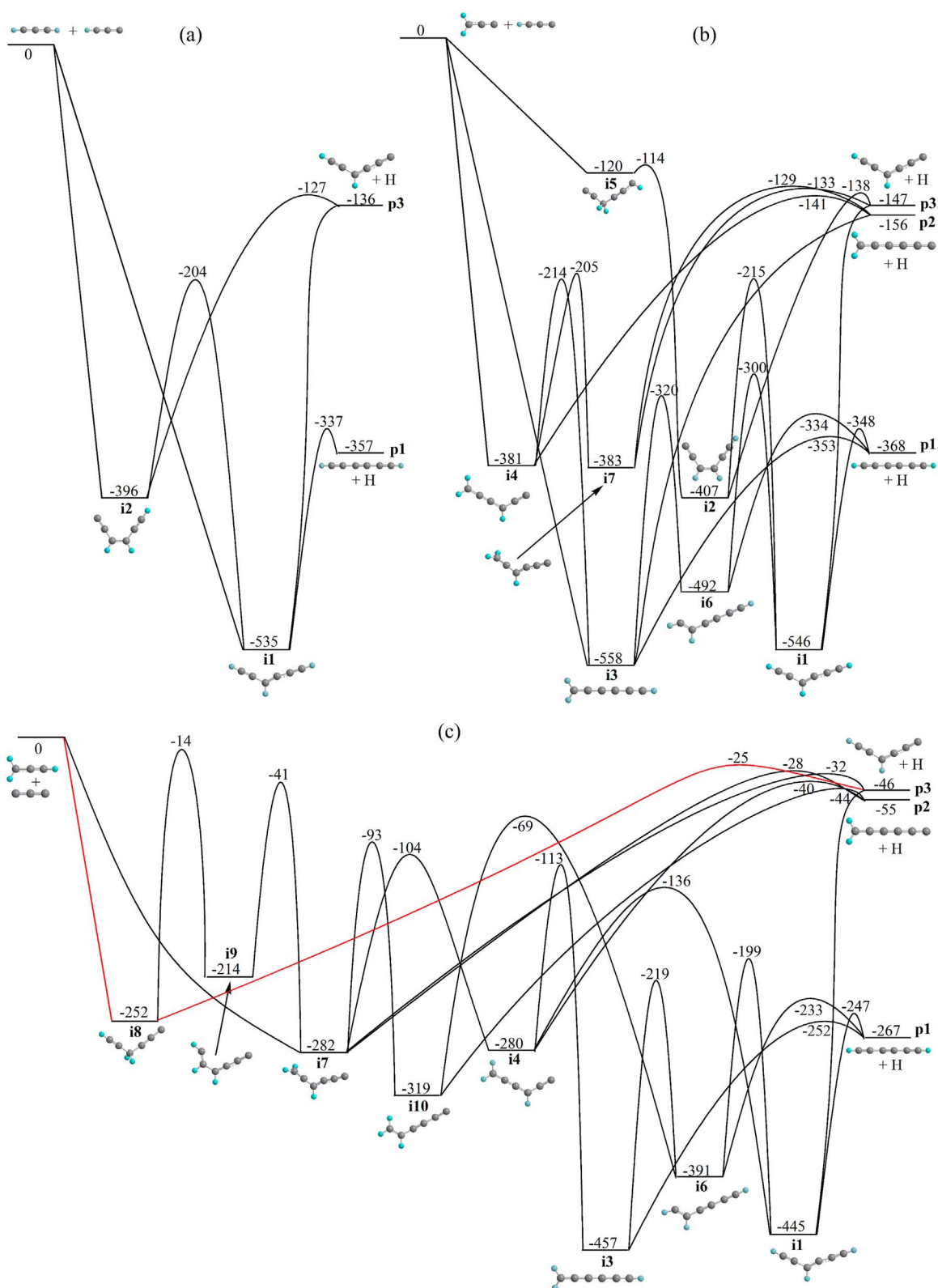


Figure 3. Potential energy surfaces (PESs) of three reactions, (a) $\text{I-HCCC} + \text{HCCCH}$, (b) $\text{I-HCCC} + \text{H}_2\text{CCC}$, and (c) $\text{C}_3 + \text{C}_3\text{H}_3$, leading to ethynylbutatrienyldiene (HCCCHCCC) and/or its isomers. Relative energies are given in kJ mol^{-1} . The most favorable pathway to p3 is shown in red.

which in turn mostly forms p1 . Statistical calculations indicate that the overall fate of i3-i5 is dictated by an eventual preparation of not ethynylbutatrienyldiene (HCCCHCCC ; p3); from i3 , triacetylene is predicted to be practically the exclusive product, and from i4 , all three C_6H_2 isomers p1-p3 can form

with the yields of 92%, 5%, and 2%, respectively, whereas from i5 , the relative yields of p1 and p3 are computed as about 98% and 2%, respectively.

Finally, the elementary gas-phase reaction of tricarbon (C_3) with the propargyl radical (C_3H_3) can be initiated by

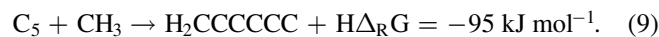
barrierless additions to the CH or CH₂ moieties of the propargyl radical leading to intermediates **i7** and **i8**, respectively, which are stabilized by 282 and 252 kJ mol⁻¹ with respect to the separated reactants. The barrierless formation of **i7** and **i8** has been verified by the scan of the PES along the reaction coordinate representing the forming C–C bond. The computed minimal energy profiles illustrated in Figure A2 in the Appendix depict a monotonous energy decrease from the reactants toward the complexes. Although tricarbon is formally a closed shell reactant, it can also be considered as a carbene as reflected through its classical Lewis structure (|C=C=C|). As illustrated in Figure 4, there is a close similarity between the highest occupied molecular orbital (HOMO) of tricarbon (C₃) representing a linear combination of lone pairs on the terminal carbon atoms and the lowest unoccupied molecular orbital (LUMO) of propargyl (C₃H₃) and a singly-occupied HOMO of C₃H₃—a π -type orbital, and LUMO of tricarbon. This similarity in symmetry properties and shape of the frontier orbitals allows for an efficient donor-acceptor interaction between the respective HOMO and LUMO of the approaching reactants and thus enables the barrierless character of the recombination reaction between the two species. From **i8**, the C–H bond rupture in the CH₂ moiety leads to ethynylbutatrienylidene (HCCCHCCC; **p3**) with the overall reaction exoergicity of 46 kJ mol⁻¹; in this case, the hydrogen atom loss barrier is 11 kJ mol⁻¹ lower than that for hydrogen atom migration leading to **i9**. As a result, the initial complex **i8** preferably dissociates to **p3**, with the computed yields of **p3** and **p1** being about 92% and 8%, respectively. While **i7** can also directly decompose to **p3** as well as to **p2**, the barriers for hydrogen migrations leading to **i4** and **i10** and, eventually, to the triacetylene product **p1** are lower than those for the hydrogen losses. This results in the predominant production of **p1** from **i7** with the computed relative yield of 99.8%.

Having provided compelling evidence on the formation of the astronomically observed ethynylbutatrienylidene (HCCCHCCC) via the barrierless and exoergic Reactions (3)–(5), we are now incorporating these elementary reactions into astrochemical models of TMC-1. The calculated abundance of ethynylbutatrienylidene (HCCCHCCC) is shown in Figure 5 (top) together with the reactants involved in Reactions (3)–(5). It can be clearly seen that the modeled peak abundance of ethynylbutatrienylidene (HCCCHCCC) of 1.2×10^{-11} , reached at a time of a few 10⁵ yr, agrees very well with the fractional abundance of $1.3 \pm 0.2 \times 10^{-11}$ derived in TMC-1 by Fuentetaja et al. (2022). The main reaction of formation of ethynylbutatrienylidene (HCCCHCCC) is Reaction (5) at a level of at least 99% (Figure 5, bottom), which is very efficient in the chemical model due to the very large abundances calculated for tricarbon (C₃), which is microwave inactive due to the lack of a permanent dipole moment, and the propargyl radical (C₃H₃), which is well constrained by observations.

5. Astrophysical Implications

The elucidation of the key synthetic pathway to ethynylbutatrienylidene (HCCCHCCC) via the bimolecular gas-phase reactions of tricarbon (C₃) with the propargyl radical (C₃H₃) has far-reaching implications to the hydrocarbon chemistry in TMC-1. First, since tricarbon is microwave inactive, the established reaction network assists in constraining the

fractional abundances of the tricarbon molecule in cold molecular clouds such as TMC-1. The fractional abundance of tricarbon (C₃) required to rationalize the presence of ethynylbutatrienylidene (HCCCHCCC) is rather high (10⁻⁵; Figure 5), which largely results from the lack of reactivity of tricarbon with atomic oxygen (Woon & Herbst 1996). The large abundance inferred for tricarbon in cold dense clouds is in contrast with the low abundances found in diffuse clouds (Roueff et al. 2002), translucent clouds (Maier et al. 2001; Oka et al. 2003; Welty et al. 2013; Schmidt et al. 2014), and in the warm star-forming region DR21(OH) (Mookerjee et al. 2012), which could arise from the very distinct physical conditions of cold dense clouds. Previous studies of reactions of tricarbon with closed shell hydrocarbons acetylene (C₂H₂), ethylene (C₂H₄), allene (H₂CCCH₂), methylacetylene (CH₃CCH), and benzene (C₆H₆) (Gu et al. 2007a; Guo et al. 2007; Mebel et al. 2007; Yang et al. 2015) reveals entrance barriers of at least 25 kJ mol⁻¹. Therefore, these elementary reactions cannot operate in cold environments such as in TMC-1. However, upon reaction with the propargyl radical (C₃H₃), a barrierless and exoergic reaction pathway was identified; this finding could be understood considering the carbene character of tricarbon and the open shell nature of the propargyl radical (Figure 4). This concept could open up a versatile pathway to exoergic reactions of tricarbon and possibly alternative carbon clusters like dicarbon (C₂), tetracarbon (C₄), and pentacarbon (C₅) with doublet hydrocarbon radicals such as methyl (CH₃; Feuchtgruber et al. 2000) forming carbene structures like vinylidene carbene (H₂CCC; Cernicharo et al. 1991a), butatrienylidene (H₂CCCC; Cernicharo et al. 1991b), pentatetraenylidene (H₂CCCCC; Cabezas et al. 2021), and hexapentaenylidene (H₂CCCCCC; Langer et al. 1997), respectively. Consequently, reactions of the tricarbon molecule, which can be formed through the elementary reactions of atomic carbon (C) with ethynyl (C₂H), methylidyne (CH) with dicarbon, and atomic carbon with acetylene (C₂H₂) (Clary et al. 2002; Kaiser 2002; Mebel & Kaiser 2002; Gu et al. 2007b; Leonori et al. 2008), with open shell hydrocarbons such as doublet radicals might provide an important source of high-energy isomers in TMC-1, whose formation pathways have been elusive so far:



Second, our investigation further provides a glimpse at reaction pathways of the resonantly stabilized propargyl radical (C₃H₃). Previous molecular beams studies revealed that the propargyl radical reacts under single-collision conditions with open shell reactants such as atomic carbon (C(³P)) and propargyl (C₃H₃) in barrierless and exoergic reactions forming diacetylene (HCCCH) plus atomic hydrogen (Kaiser et al. 1997) and the phenyl radical (C₆H₅) along with its acyclic isomers plus atomic hydrogen (Zhao et al. 2022). However, in cold molecular clouds at 10 K, the propargyl radical does not react with closed shell reactants such as acetylene (C₂H₂), ethylene

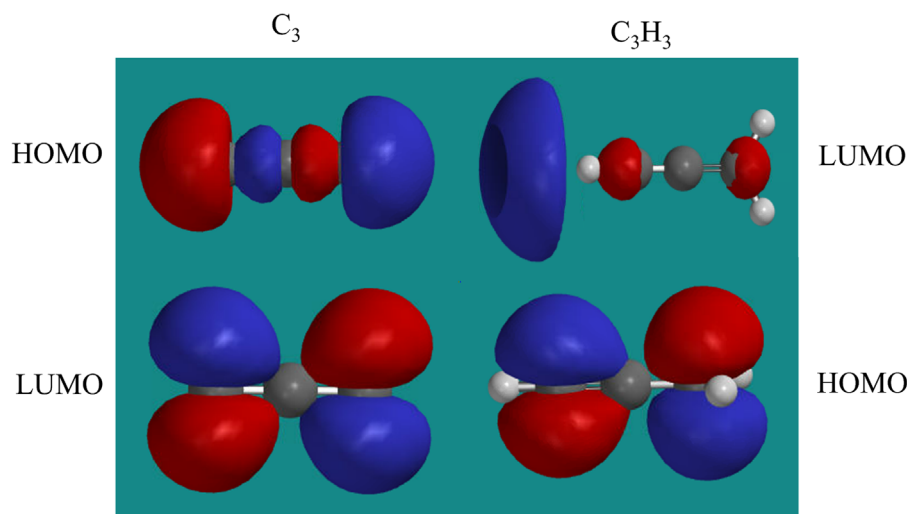


Figure 4. Molecular orbitals involved in the barrierless addition of the tricarbon molecule to the propargyl radical.

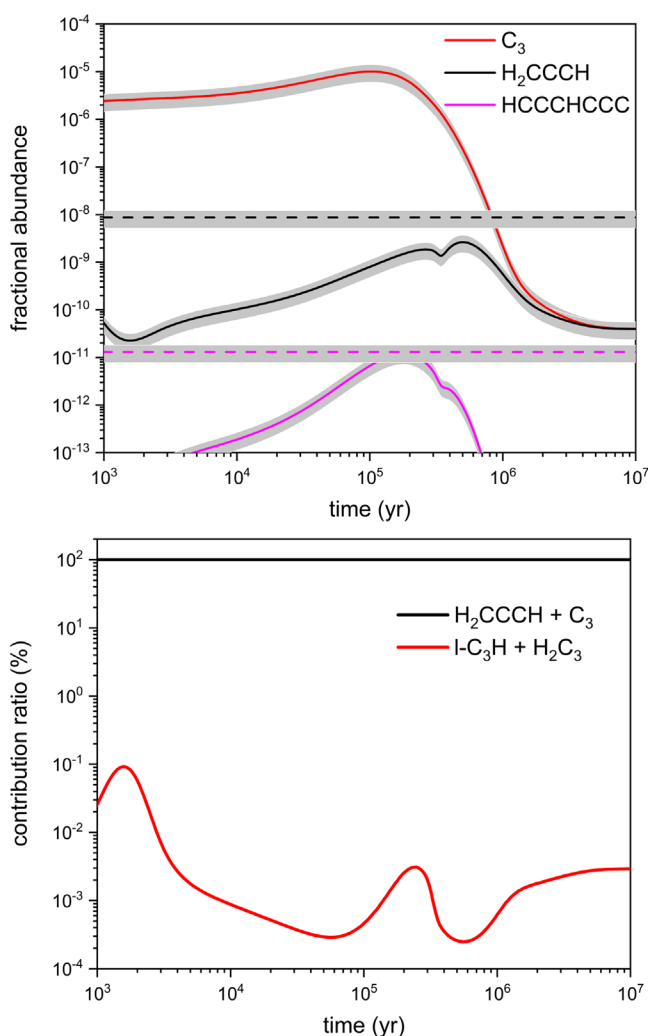


Figure 5. Upper panel: calculated fractional abundances of ethynylbutatrienyldene (HCCCHCCC) along with the tricarbon (C_3) and propargyl radical reactants (C_3H_3). Observed values, indicated by horizontal dotted lines, were taken from Agúndez et al. (2022) for propargyl (C_3H_3) and Fuentetaja et al. (2022) for ethynylbutatrienyldene (HCCCHCCC). Lower panel: contributions of the reactions of $I\text{-HCCC} + \text{HCCCH}$ and $C_3 + C_3H_3$ leading to ethynylbutatrienyldene (HCCCHCCC).

(C_2H_4), allene (H_2CCCH_2), methylacetylene (CH_3CCH), and benzene (C_6H_6) due to insurmountable barriers of addition of at least 40 kJ mol^{-1} .⁴ The tricarbon reactant explored here represents a closed shell molecule; nevertheless, the carbene character of the terminal carbon atoms and hence the electron deficient nature of these carbon centers open the door for a barrierless addition of the propargyl radical, as verified by electronic structure calculations (Figure 3). Overall, the facile formation of ethynylbutatrienyldene (HCCCHCCC; X^1A') via the elementary gas-phase reaction of tricarbon with the propargyl radical challenges conventional wisdom that tricarbon represents a chemically “dead” species in molecular clouds, and its reactions with doublet radicals (CH , CH_3 , C_2H , C_2H_3 , C_2H_5 , C_3H , C_3H_5 , C_4H) and triplet biradicals like propargylene (HCCCH) and pentadienyldene (HCCCCCH) might form either higher carbon clusters ($C_4\text{--}C_6$) and/or high-energy hydrocarbon isomers in deep space.

This work was supported by the U.S. Department of Energy, Basic Energy Sciences under grants DE-FG02-03ER15411 and DE-FG02-04ER15570 to the University of Hawaii and to Florida International University, respectively, by the European Research Council under grant 610256 (NANOCOSMOS), and by the Spanish Ministerio de Ciencia e Innovación under grants PID2019-107115GB-C21 and PID2019-106110GB-I00.

Appendix

Figures A1 and A2 illustrating respectively the combined C_6H_3 PES and minimal potential energy profiles for the initial recombination reaction steps of the $C_3 + C_3H_3$ reaction.

⁴ <https://kinetics.nist.gov>

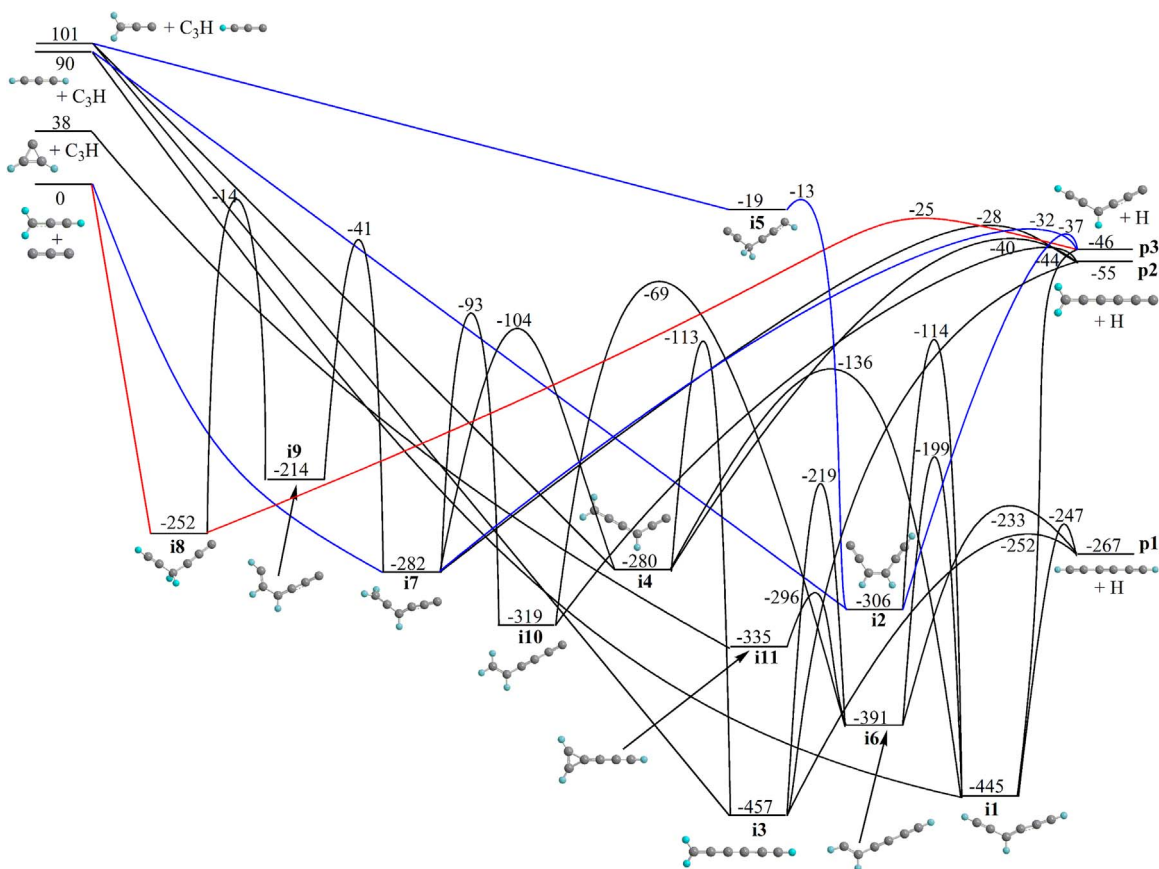


Figure A1. Combined potential energy diagram for the 1-CCCH + C₃H₂ and C₃ + C₃H₃ reactions accessing the C₆H₃ PES. Relative energies are shown in kJ mol⁻¹ with respect to C₃ + C₃H₃. The red and blue lines respectively show the major and minor pathways leading to the formation of ethynylbutatrienylidene (HCCCHCCC, **p3**) plus atomic hydrogen.

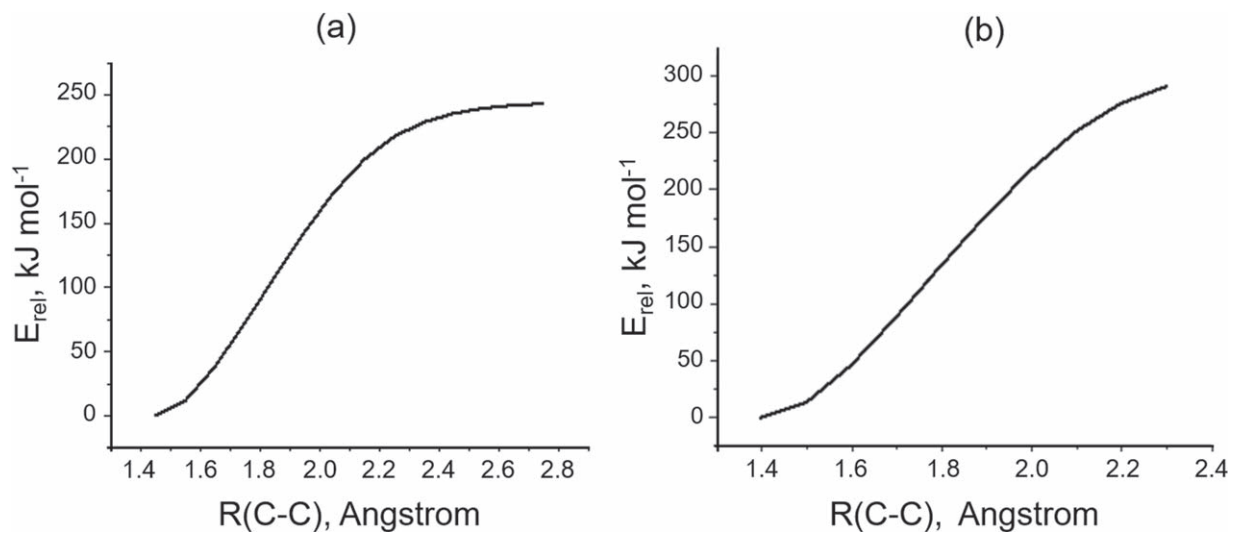



Figure A2. Minimal potential energy profiles for the initial recombination reaction steps C₃ + C₃H₃ → **i8** (a) and C₃ + C₃H₃ → **i7** (b) calculated at the ω B97XD/cc-pVTZ level of theory.

Table A1

Calculated Product Branching Fractions (%) at Zero Collision Energy under Single-collision Conditions

Reaction	Initial Complex	p1 + H	p2 + H	p3 + H
I-HCCC + HCCCH	i1	99.98	0.00	0.02
	i2	97.87	0.00	2.13
I-HCCC + H ₂ CCC	i3	100.00	0.00	0.00
	i4	92.15	5.40	2.45
	i5	98.15	0.00	1.85
C ₃ + C ₃ H ₃	i7	99.78	0.18	0.04
	i8	7.67	0.02	92.31

ORCID iDsAlexander M. Mebel  <https://orcid.org/0000-0002-7233-3133>Marcelino Agúndez  <https://orcid.org/0000-0003-3248-3564>José Cernicharo  <https://orcid.org/0000-0002-3518-2524>Ralf I. Kaiser  <https://orcid.org/0000-0002-7233-7206>**References**

- Adler, T. B., Knizia, G., & Werner, H.-J. 2007, *JChPh*, **127**, 221106
- Agúndez, M., Cabezas, C., Tercero, B., et al. 2021, *A&A*, **647**, L10
- Agúndez, M., Marcelino, N., Cabezas, C., et al. 2022, *A&A*, **657**, A96
- Balucani, N., Asvany, O., Chang, A. H. H., et al. 1999, *JChPh*, **111**, 7457
- Berteloite, C., Le Picard, S. D., Balucani, N., Canosa, A., & Sims, I. R. 2010, *PCCP*, **12**, 3677
- Cabezas, C., Tercero, B., Agúndez, M., et al. 2021, *A&A*, **650**, L9
- Cernicharo, J., Agúndez, M., Cabezas, C., et al. 2021b, *A&A*, **647**, L2
- Cernicharo, J., Agúndez, M., Kaiser, R. I., et al. 2021a, *A&A*, **652**, L9
- Cernicharo, J., Gottlieb, C. A., Guélin, M., et al. 1991a, *ApJ*, **368**, L39
- Cernicharo, J., Gottlieb, C. A., Guélin, M., et al. 1991b, *ApJ*, **368**, L43
- Chai, J.-D., & Head-Gordon, M. 2008, *PCCP*, **10**, 6615
- Clary, D. C., Buonomo, E., Sims, I. R., et al. 2002, *JPCA*, **106**, 5541
- Cooke, I. R., Gupta, D., Messinger, J. P., & Sims, I. R. 2020, *ApJL*, **891**, L41
- Dunning, T. H. 1989, *JChPh*, **90**, 1007
- Eyring, H., Lin, S. H., & Lin, S. M. 1980, *Basic Chemical Kinetics* (New York: Wiley)
- Feuchtgruber, H., Helmich, F. P., van Dishoeck, E. F., & Wright, C. M. 2000, *ApJL*, **535**, L111
- Frisch, M. J., Trucks, G. W., Schlegel, H. B., et al. 2016, *Gaussian 16, Revision B.01* (Wallingford, CT: Gaussian Inc.)
- Fuentetaja, R., Agúndez, M., Cabezas, C., et al. 2022, *A&A*, **667**, L4
- Gu, X., Guo, Y., Mebel, A. M., & Kaiser, R. I. 2007a, *CPL*, **449**, 44
- Gu, X., Guo, Y., Zhang, F., & Kaiser, R. I. 2007b, *JPCA*, **111**, 2980
- Gu, X., Kim, Y. S., Kaiser, R. I., et al. 2009, *PNAS*, **106**, 16078
- Guo, Y., Gu, X., Zhang, F., Mebel, A. M., & Kaiser, R. I. 2007, *PCCP*, **9**, 1972
- He, C., Yang, Z., Doddipatla, S., et al. 2022, *PCCP*, **24**, 26499
- Jones, B. M., Zhang, F., Kaiser, R. I., et al. 2011, *PNAS*, **108**, 452
- Kaiser, R. I. 2002, *ChRv*, **102**, 1309
- Kaiser, R. I., & Balucani, N. 2001, *AcChR*, **34**, 699
- Kaiser, R. I., & Hansen, N. 2021, *JPCA*, **125**, 3826
- Kaiser, R. I., Sun, W., Suits, A. G., & Lee, Y. T. 1997, *JChPh*, **107**, 8713
- Kaiser, R. I., Zhao, L., Lu, W., et al. 2022, *PCCP*, **24**, 25077
- Kislov, V. V., Nguyen, T. L., Mebel, A. M., Lin, S. H., & Smith, S. C. 2004, *JChPh*, **120**, 7008
- Knizia, G., Adler, T. B., & Werner, H.-J. 2009, *JChPh*, **130**, 054104
- Landera, A., Krishtal, S. P., Kislov, V. V., Mebel, A. M., & Kaiser, R. I. 2008, *JChPh*, **128**, 214301
- Langer, W. D., Velusamy, T., Kuiper, T. B. H., et al. 1997, *ApJL*, **480**, L63
- Leonori, F., Petrucci, R., Segoloni, E., et al. 2008, *JPCA*, **112**, 1363
- Loison, J.-C., Agúndez, M., Wakelam, V., et al. 2017, *MNRAS*, **470**, 4075
- Maier, J. P., Lakin, N. M., Walker, G. A., & Bohlender, D. A. 2001, *ApJ*, **553**, 267
- Maksyutenko, P., Zhang, F., Gu, X., & Kaiser, R. I. 2011, *PCCP*, **13**, 240
- McCarthy, M. C., & Thaddeus, P. 2002, *ApJL*, **569**, L55
- McElroy, D., Walsh, C., Markwick, A. J., et al. 2013, *A&A*, **550**, A36
- McGuire, B. A., Burkhardt, A. M., Kalenskii, S., et al. 2018, *Sci*, **359**, 202
- McGuire, B. A., Loomis, R. A., Burkhardt, A. M., et al. 2021, *Sci*, **371**, 1265
- Mebel, A. M., & Kaiser, R. I. 2002, *CPL*, **360**, 139
- Mebel, A. M., Kim, G.-S., Kislov, V. V., & Kaiser, R. I. 2007, *JPCA*, **111**, 6704
- Mookerjee, B., Hassel, G. E., Gerin, M., et al. 2012, *A&A*, **546**, A75
- Nguyen, T. L., Mebel, A. M., & Kaiser, R. I. 2001, *JPCA*, **105**, 3284
- Oka, T., Thorburn, J. A., McCall, B. J., et al. 2003, *ApJ*, **582**, 823
- Parker, D. S. N., Zhang, F., Kim, Y. S., et al. 2012, *PNAS*, **109**, 53
- Roueff, E., Felenbok, P., Black, J. H., & Gry, C. 2002, *A&A*, **384**, 629
- Schmidt, M., Krelowski, J., Galazutdinov, G., et al. 2014, *MNRAS*, **441**, 1134
- Sims, I. R., & Smith, I. W. M. 1995, *ARPC*, **46**, 109
- Suutarinen, A., Geppert, W. D., Harju, J., et al. 2011, *A&A*, **531**, A121
- Thaddeus, P., Gottlieb, C. A., Hjalmarsen, A., et al. 1985, *ApJL*, **294**, L49
- Tucker, K. D., Kutner, M. L., & Thaddeus, P. 1974, *ApJL*, **193**, L115
- Turner, A. M., & Kaiser, R. I. 2020, *AcChR*, **53**, 2791
- Vakhtin, A. B., Heard, D. E., Smith, I. W. M., & Leone, S. R. 2001, *CPL*, **344**, 317
- Wakelam, V., Loison, J.-C., Herbst, E., et al. 2015, *ApJS*, **217**, 20
- Welty, D. E., Howk, J. C., Lehner, N., & Black, J. H. 2013, *MNRAS*, **428**, 1107
- Werner, H. J., Knowles, P. J., Knizia, G., et al. 2021, *MOLPRO*, Version 2021 (UK: Univ. College Cardiff Consultants Ltd)
- Wilson, A. V., Parker, D. S. N., Zhang, F., & Kaiser, R. I. 2012, *PCCP*, **14**, 477
- Woon, D. E., & Herbst, E. 1996, *ApJ*, **465**, 795
- Yang, T., Muzangwa, L., Kaiser, R. I., Jamal, A., & Morokuma, K. 2015, *PCCP*, **17**, 21564
- Zhang, J., & Valeev, E. F. 2012, *J Chem Theory Comput*, **8**, 3175
- Zhao, L., Lu, W., Ahmed, M., et al. 2021, *SciA*, **7**, eabf0360